JOURNAL OF VIROLOGY, Mar. 1994, p. 1551–1563
0022-538X/94/$04.00+0

Vol. 68, No. 3

# Influenza A Virus $M_2$ Ion Channel Protein: a Structure-Function Analysis

LESLIE J. HOLSINGER,[1] DEEPALI NICHANI,[1] LAWRENCE H. PINTO,[2] AND ROBERT A. LAMB[1,3]*

*Department of Biochemistry, Molecular Biology and Cell Biology,[1] Department of Neurobiology and Physiology,[2] and Howard Hughes Medical Institute,[3] Northwestern University, Evanston, Illinois 60208-3500*

Received 11 October 1993/Accepted 30 November 1993

**A structure-function analysis of the influenza A virus $M_2$ ion channel protein was performed. The $M_2$ protein of human influenza virus A/Udorn/72 and mutants containing changes on one face of the putative α helix of the $M_2$ transmembrane (TM) domain, several of which lead to amantadine resistance when found in virus, were expressed in oocytes of *Xenopus laevis*. The membrane currents of oocytes expressing mutant $M_2$ ion channels were measured at both normal and low pH, and the amantadine-resistant mutant containing the change of alanine at residue 30 to threonine was found to have a significantly attenuated low pH activation response. The specific activity of the channel current of the amantadine-resistant mutants was investigated by measuring the membrane current of individual oocytes followed by quantification of the amount of $M_2$ protein expressed in these single oocytes by immunoblotting analysis. The data indicate that changing residues on this face of the putative α helix of the $M_2$ TM domain alters properties of the $M_2$ ion channel. Some of the $M_2$ proteins containing changes in the TM domain were found to be modified by addition of an N-linked carbohydrate chain at an asparagine residue that is membrane proximal and which is not modified in the wild-type $M_2$ protein. These N-linked carbohydrate chains were further modified by addition of polylactosaminoglycan. A glycosylated $M_2$ mutant protein ($M_2$+V, A30T) exhibited an ion channel activity with a voltage-activated, time-dependent kinetic component. Prevention of carbohydrate addition did not affect the altered channel activity. The ability of the $M_2$ protein to tolerate deletions in the TM domain was examined by expressing three mutants ($del_{29-31}$, $del_{28-31}$, and $del_{27-31}$) containing deletions of three, four, and five residues in the TM domain. No ion channel activity was detected from expression of $M_2$ $del_{29-31}$ and $del_{27-31}$, whereas expression of $M_2$ $del_{28-31}$ resulted in an ion channel activity that was activated by hyperpolarization (and not low pH) and was resistant to amantadine block. Examination of the oligomeric form of $M_2$ $del_{28-31}$ indicated that the oligomer is different from wild-type $M_2$, and the data were consistent with $M_2$ $del_{28-31}$ forming a pentamer.**

The influenza A virus $M_2$ protein is a small (97-amino-acid residue) transmembrane (TM) protein which is encoded by a spliced mRNA derived from genomic RNA segment 7 (20, 23). While the $M_2$ protein is abundantly expressed at the plasma membrane of virus-infected cells, it is a comparatively minor component of virions (24, 44). The $M_2$ protein contains three domains: a 24-residue N-terminal extracellular domain, a 19-residue signal anchor TM domain, and a 54-residue cytoplasmic tail (16, 24). Minimally, the $M_2$ protein forms a homotetramer composed of a pair of disulfide-linked dimers or a disulfide-linked tetramer, with the disulfide bonds acting to stabilize the oligomer (15, 38).

The $M_2$ protein has been proposed to function as an ion channel that permits ions to enter endocytosed virions and to function as a modulator of pH in intracellular compartments (11, 38). Direct evidence that the $M_2$ protein has ion channel activity was obtained by expressing the $M_2$ protein in oocytes of *Xenopus laevis* and measuring membrane currents (32). The $M_2$ ion channel activity was found to be blocked by the anti-influenza virus drug amantadine hydrochloride, thereby providing direct evidence for the mechanism of action for the drug (32). Influenza virus mutants resistant to amantadine contain amino acid changes in the $M_2$ protein TM domain (12), and when the altered $M_2$ proteins were expressed in oocytes, they exhibited ion channel activities that were not affected by the drug (32). The $M_2$ ion channel was found to be permeable to $Na^+$ ions, and it is likely that this monovalent cation conductance also extends to protons (32). Specific changes in the $M_2$ protein TM domain altered the kinetics and ion selectivity of the channel, providing strong evidence that the $M_2$ TM domain constitutes the pore of the channel (32). This notion is supported by the finding that when a peptide corresponding to the $M_2$ protein TM domain was incorporated into planar membranes, a proton translocation susceptible to block by amantadine could be detected (5). The $M_2$ ion channel activity was found to be regulated by changes in pH (32, 41), with the channel being activated at the lowered pH found intralumenally in endosomes and the *trans* Golgi network.

In the life cycle of influenza virus, the $M_2$ protein ion channel activity is thought to function at an early stage between the steps of virus penetration and uncoating. It is generally believed that once the virion particle has been endocytosed, the virion-associated ion channel permits the flow of ions from the endosome into the virion interior to disrupt protein-protein interactions and release the ribonucleoprotein structure from the membrane (matrix) ($M_1$) protein (reviewed in reference 14). In addition, for some strains of influenza virus which have a hemagglutinin (HA) that is cleaved intracellularly and a high pH optimum of fusion (e.g., fowl plague virus [FPV] Rostock), the $M_2$ ion channel is thought to function in the *trans* Golgi network to modulate pH such that it remains above the threshold needed to induce the acid pH transition of HA (2, 3, 9, 10, 28, 37, 39).

The $M_2$ protein sequence does not indicate any obvious

* Corresponding author. Mailing address: Department of Biochemistry, Molecular Biology and Cell Biology, Northwestern University, 2153 N. Campus Dr., Evanston, IL 60208-3500. Phone: (708) 491-5433. Fax: (708) 491-2467. Electronic mail address: ralamb@nwu.edu

homology with other proteins found in the data base of protein sequences. In addition, the $M_2$ protein is a minimalistic ion channel, as it contains only a single TM domain, in comparison with the majority of ion channels (reviewed in reference 26). Thus, we were interested in performing a detailed structure-function analysis of the $M_2$ protein. We describe here properties of altered $M_2$ molecules expected to be resistant to amantadine, properties of altered $M_2$ molecules that are glycosylated, and properties of altered $M_2$ molecules containing deletions in the TM domain. The properties of these altered $M_2$ molecules are discussed in terms of possible ion channel molecular architecture.

## MATERIALS AND METHODS

**Site-specific mutagenesis, construction of recombinant plasmids, and in vitro RNA synthesis.** The cDNA to influenza virus A/Udorn/72 mRNA (16, 45) was cloned either into the *Bam*HI site of the replicative form of M13mp19 and used as a template DNA for site-specific mutagenesis (15) or into the *Bam*HI site of pGEM3Zf(+) and used as a template for phagemid-based mutagenesis (31). Oligonucleotides were synthesized by the Northwestern University Biotechnology Facility on a DNA synthesizer (model 380B; Applied Biosystems, Inc., Foster City, Calif.). Mutant cDNAs encoding the altered $M_2$ genes were excised from the replicative form of M13 by *Bam*HI digestion and subcloned into the *Bam*HI site of a pGEM3 vector such that mRNA sense transcripts could be generated by using the bacteriophage T7 RNA polymerase promoter and T7 polymerase. The nucleotide sequences of the altered cDNAs in both the pGEM3 vector and pGEM3Zf(+) phagemid vector were confirmed by dideoxynucleotide chain-terminating sequencing (34). For in vitro transcription, plasmid DNAs were linearized downstream of the T7 promoter and the $M_2$ cDNA with *Xba*I. In vitro synthesis and quantitation of $^{7m}$G(5′)ppp(5′)G-capped mRNA was carried out as described previously (32).

**Microinjection and culture of oocytes.** Ovarian lobules from *X. laevis* females (Nasco, Fort Atkinson, Wis.) were surgically removed and treated with collagenase B (2 mg/ml; Boehringer Mannheim Biochemicals, Indianapolis, Ind.) (32). Selected oocytes (stages V and VI) were injected with 50 nl of RNA (1.0 μg/μl) by using a 20-μm-diameter glass pipette, and oocytes were maintained in ND96 (32) at 17°C.

**Metabolic labeling of injected oocytes, immunoblotting analysis, immunoprecipitation, and SDS-PAGE.** For immunoprecipitations, oocytes were incubated in ND96 supplemented with [$^{35}$S]methionine (250 μCi/ml; Amersham Corp., Arlington Heights, Ill.) from 24 to 48 h postinjection. Labeled oocytes were homogenized in, per oocyte, 75 μl of radioimmunoprecipitation assay (RIPA) buffer containing 50 mM iodoacetamide and a cocktail of protease inhibitors (phenylmethylsulfonyl fluoride, aprotinin, antipain, pepstatin A, leupeptin, and chymostatin) (30), and extracts were immunoprecipitated (21) with $M_2$-specific 14C2 monoclonal antibody ascites fluid (44). Samples were analyzed by sodium dodecyl sulfate (SDS)-polyacrylamide gel electrophoresis (PAGE) on 17.5% polyacrylamide–4 M urea gels and processed for fluorography and autoradiography as described previously (19). For immunoblotting of single oocyte lysates, individual unlabeled oocytes were lysed in 100 μl of RIPA buffer and extracted once with 1,1,2-trichlorotrifluoroethane to remove yolk and pigment proteins. Five to 10 μl of lysates was analyzed on 17.5% polyacrylamide–4 M urea gels and electrotransferred to polyvinylidene difluoride membranes (Millipore, Bedford, Mass.) by using a Trans-Blot semidry transfer cell (Bio-Rad, Richmond, Calif.). Filters were incubated with 5% powdered milk–0.3% Tween 20–phosphate-buffered saline (PBS) for 60 min to block nonspecific sites and then incubated for 60 min with a 1:3,000 dilution of $M_2$-specific 14C2 ascites fluid (44). Filters were washed in PBS–0.3% Tween 20 and incubated for 60 min with a 1:1,000 dilution of horseradish peroxidase-conjugated goat anti-mouse immunoglobulin G secondary antibody (Cappel, Organon Teknika, Malvern, Pa.). Blots were extensively washed in PBS with 0.3% Tween 20, and the $M_2$ protein immune complex was detected with the ECL (enhanced chemiluminescence) system (Amersham International, Arlington Heights, Ill.). Autoradiography was performed by using preflashed X-ray film (25) and quantitated by laser scanning densitometry on an LKB Ultroscan XL densitometer (Pharmacia-LKB, Piscataway, N.J.). For quantification of blots, 50 to 400 pg of purified $M_2$ protein, the precise amount depending on the $M_2$ mutant under analysis, was run with all samples in order to generate a standard curve. $M_2$ protein was purified from detergent lysates of influenza virus A/Udorn/72-infected CV-1 cells by immunoaffinity chromatography using $M_2$-specific purified 14C2 immunoglobulin G coupled to CNBr-activated Sepharose 4B (15).

**Endo-β-galactosidase digestions and tunicamycin treatment.** Proteins were immunoprecipitated, and protein A-Sepharose antibody-antigen complexes were boiled in 20 μl of 10 mM Tris (pH 7.4)–0.2% SDS for 4 min, diluted with an equal volume of assay buffer (0.1 M sodium acetate [pH 5.5], 70 mM NaCl), and incubated with 20 mU of endo-β-galactosidase (ICN ImmunoBiologicals, Costa Mesa, Calif.) suspended in 20 μl of assay buffer for 16 h at 37°C. For tunicamycin treatment of oocytes, mRNAs were mixed with tunicamycin (final concentration of 40 μg/ml, made from a 1-mg/ml stock in dimethyl sulfoxide; Calbiochem-Behring Corp., La Jolla, Calif.) prior to injection, and injected oocytes were incubated in ND96 contain 2 μg of tunicamycin per ml during metabolic labeling. Oocytes were then homogenized, and extracts were immunoprecipitated as described above.

**Chemical cross-linking.** For analysis of the oligomeric form of wild-type (wt) $M_2$ and $M_2$ $del_{28-31}$ proteins, homobifunctional cross-linking reagents were used. The proteins were expressed in CV-1 cells by using simian virus 40 (SV40) recombinants. Both the wt and mutant $M_2$ cDNAs were subcloned into the *Bam*HI site of the SV40 VP1 replacement vector pSV73E/K (45) such that the $M_2$ cDNA was under the control of the SV40 late-region promoter, splicing, and polyadenylation sites. SV40 recombinant virus stocks were produced essentially as described previously (22). SV40 recombinant virus-infected CV-1 cells were labeled with [$^{35}$S]cysteine (100 μCi/ml) in Dulbecco modified Eagle medium deficient in cysteine from 45 to 48 h postinfection. Cells were lysed in 1% Nonidet P-40–50 mM Tris-HCl (pH 8.0)–100 mM NaCl–50 mM iodoacetamide and incubated with and without dithio-bis (succinimidylpropionate) (DSP; final concentration of 1 mg/ml, from a 50-mg/ml stock in dimethyl sulfoxide; Pierce Chemical Co., Rockford, Ill.) for 30 min at 4°C. Reactions were stopped by addition of glycine (final concentration, 60 mM). Lysates were clarified at 100,000 × *g* and immunoprecipitated as described above. In addition, cross-linking was performed on intact cells. Monolayers of radioactively labeled virus-infected cells were washed with cold PBS and incubated with ethylene glycol-bis(succinimidlysuccinate) (EGS; final concentration of 1 mg/ml, from a 50 mg/ml stock in dimethyl sulfoxide; Pierce) and incubated overnight at 4°C. Excess cross-linker was neutralized with 60 mM glycine; monolayers were washed in PBS, lysed in 1% Nonidet P-40–50 mM Tris-HCl (pH 8.0)–100 mM NaCl–50 mM iodoacetamide,

clarified at 100,000 × *g*, and immunoprecipitated as described above.

**Sucrose density gradient sedimentation analysis.** Sedimentation analysis of the oligomeric forms of $M_2$ was performed essentially as described previously (15, 27), with the following modifications. Recombinant SV40-infected CV-1 cells were labeled with [$^{35}$S]cysteine at 48 h postinfection for 2 h and lysed in MNT buffer (20 mM morpholineethanesulfonic acid [MES], 30 mM Tris-HCl, 100 mM NaCl [pH 7.0], 1% Triton X-100, 50 mM iodoacetamide, protease inhibitors). Lysates were cross-linked with DSP (1 mg/ml) as described above, and nuclei and cell debris were removed by centrifugation (55,000 rpm, 10 min, 4°C) in a TLA 100.2 rotor (Beckman Instruments Inc., Palo Alto, Calif.). Lysates were layered onto an 11-ml continuous 5 to 15% (wt/vol) sucrose gradient in MNT buffer–0.1% Triton X-100 that overlaid a 0.75-ml 60% sucrose cushion. Sedimentation was done in an SW41 rotor (Beckman) at 38,000 rpm at 20°C for 24 h. Twenty-four 0.5-ml fractions were collected dropwise from the bottom of the tube, diluted in RIPA buffer, and immunoprecipitated as described above.

**Indirect immunofluorescence microscopy.** Oocytes were injected with $M_2$ mRNAs and incubated for 48 to 72 h at 17°C as described above. Oocytes were frozen by plunging into isopentane cooled to −170°C over liquid nitrogen and then embedded, and 10-μm sections were cut on a cryostat (Bright Instrument Co., Huntingdon, England) at −22°C. Sections were collected on gelatin-coated slides and air dried. Dried sections were fixed in 1% formaldehyde and stained with antibody (44). Fixed sections were stained with $M_2$-specific 14C2 ascites fluid (diluted 1:300 in PBS–1% bovine serum albumin) and incubated with fluorescein isothiocyanate (FITC)-conjugated goat anti-mouse secondary antibody. Photomicroscopy was performed by using a Nikon Microphot-FXA microscope (Nikon, Inc., Melville, N.Y.). All photographic exposure times were equivalent.

**Electrophysiological recordings.** Whole-cell currents were recorded from oocytes 49 to 72 h after mRNA injection with a two-electrode voltage clamp apparatus (32). Amantadine hydrochloride (10 mM stock in water; Sigma Chemical Co., St. Louis, Mo.) was diluted as indicated.

## RESULTS

**Expression in oocytes of mutant $M_2$ proteins with changes on one face of the putative α-helical TM domain.** If the $M_2$ protein TM domain is modeled as an α helix, $M_2$ protein residues V-27, A-30, S-31, G-34, L-38, and W-41 lie on the same face of the α helix, and mutations at residues V-27, A-30, S-31, G-34, and L-38 lead to ion channels with altered activity and altered susceptibility to amantadine (9, 32, 41). To begin a structure function analysis of the residues in the human influenza virus (A/Udorn/72) $M_2$ protein TM domain, the pH activation response of the amantadine-resistant mutants V27A, V27S, A30T, S31N (32) was tested, and the amantadine sensitivity and pH activation of additional mutations in the Udorn $M_2$ protein containing the changes V27T, A30P, and G34E, and W41A (Fig. 1A) were examined. The changes I27S, I27T, I27A, V27A, V27D, A30E, A30P, S31N, and G34E have been found to arise naturally in amantadine-resistant viruses of avian influenza viruses, FPV strains Rostock (A/chicken/Germany/34) and Weybridge (A/chicken/Germany/27) (9, 12). The changes V27T and V27S in Udorn $M_2$ protein are artificial, but as the changes I27T, I27S, and V27A are found naturally (see above), it was of interest to begin to examine the plasticity of the channel structure at this residue. We also changed the tyrosine 41 residue (mutant W41A) on this face of the putative α helix of the $M_2$ protein TM domain because aromatic residues in the channel pore are thought to play an important role in $K^+$ channel conductances (13, 18).

To examine the synthesis of the $M_2$ protein point mutants, oocytes were injected with synthetic mRNA transcripts and metabolically labeled with [$^{35}$S]methionine for 24 h. $M_2$ proteins were immunoprecipitated, and the polypeptides were analyzed by SDS-PAGE (Fig. 1B and C). Under reducing conditions (in the presence of dithiothreitol [DTT]; Fig. 1B), species of $M_r$ ~15,000 could be detected for each of the point mutants (data for W41A not shown). For $M_2$ A30P and G34E, an additional band of $M_r$ ~18,000 could be readily identified, and for mutants A30P and G34E, slowly migrating heterogeneous populations of molecules (~30 to 50 kDa) could be observed. As discussed below, these additional $M_2$-specific species are due to a modification of $M_2$ molecules by the addition of N-linked carbohydrate chains and their subsequent modification with polylactosaminoglycan. Under nonreducing conditions, the mutants were found to form a mixture of disulfide-linked dimers (~30 kDa) and disulfide-linked tetramers (~60 kDa) (Fig. 1C).

From extensive studies, particularly of viral integral membrane proteins, the concept has emerged that correct folding and oligomerization of membrane proteins is a prerequisite for transport through the exocytotic pathway. Molecules which are malfolded are blocked in transport in the endoplasmic reticulum (reviewed in reference 4). Therefore, it was necessary to establish whether the altered $M_2$ proteins were expressed at the plasma membrane of oocytes, as failure of a channel polypeptide to be transported to the plasma membrane would yield a phenotype indistinguishable from that of a molecule expressed at the cell surface that lacked ion channel activity. Frozen sections of oocytes expressing $M_2$ V27T, A30P, and G34E were stained with an $M_2$ ectodomain-specific monoclonal antibody and FITC-labeled secondary antibody, and a characteristic surface staining pattern was observed (Fig. 2), indicating proper transport to the oocyte plasma membrane. The surface expression of the wt $M_2$ protein and the other mutants indicated in Fig. 1 has been shown previously (32).

**Amantadine block and pH activation of $M_2$ protein ion channel activity.** To determine the amantadine sensitivity and pH activation of altered $M_2$ proteins expressed in oocytes of *X. laevis*, a two-electrode voltage clamp procedure was used, and total membrane currents were measured. The currents were studied by holding the membrane voltage at −40 mV and hyperpolarizing the membrane with step voltage clamp pulses from −130 to −60 mV. The peak amplitudes of inward current following an activating voltage of −130 mV in normal Barth's solution at pH 7.5 and 6.2 are shown in Table 1. For all measurements described herein, the small endogenous current exhibited by control oocytes injected with antisense RNA was subtracted from the measured current to yield the current reported. Although oocytes expressing both the wt and mutant $M_2$ proteins had only small membrane currents at neutral pH, the current amplitude increased an average of eightfold when the current was measured at pH 6.2. We noted that oocytes expressing one mutant polypeptide, $M_2$ A30P, had essentially no current at either pH 7.5 or pH 6.2, suggesting this protein does not have functional ion channel activity. When oocytes were bathed in Barth's solution containing 100 μM amantadine at pH 7.5, the current of oocytes expressing the wt $M_2$ protein was attenuated, whereas the currents of oocytes expressing $M_2$ V27A, V27S, A30T, S31N, and G34E were resistant to the drug (data not shown). Similarly, following activation at pH 6.2, the current of oocytes expressing the wt $M_2$ protein was still sensitive to amantadine, whereas the

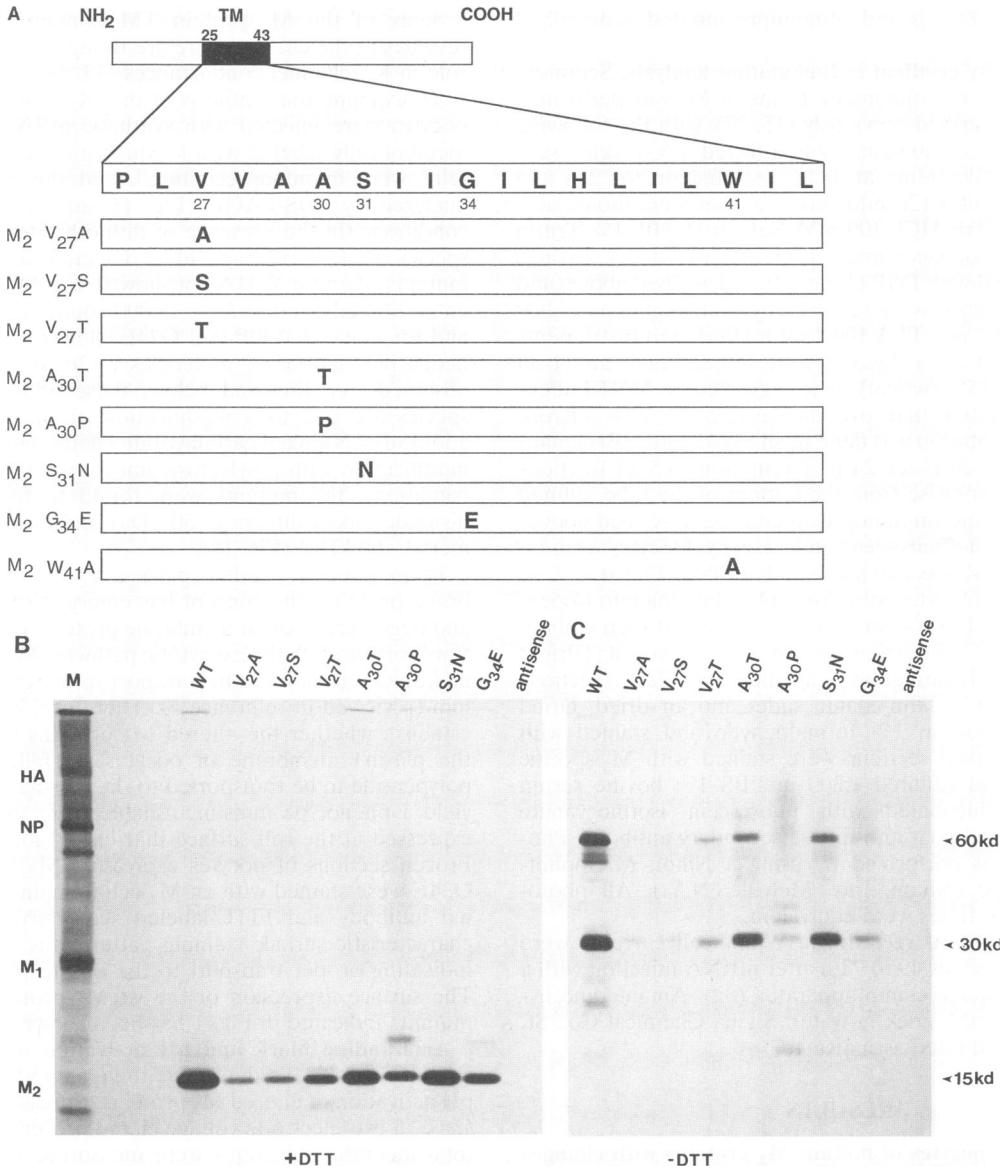


FIG. 1. Construction and expression of influenza virus wt $M_2$ and mutant $M_2$ polypeptides in oocytes. (A) Schematic diagram of the influenza virus $M_2$ protein and its hydrophobic TM domain residues 25 to 43. The amino acid sequence of the TM domain is shown in the expanded section of the diagram, using the single-letter code. The mutants $M_2$ V27A, V27S, V27T, A30T, A30P, S31N, G34E, and W41A were constructed as described in Materials and Methods. (B and C) Expression of wt $M_2$ and mutant $M_2$ polypeptides in oocytes of *X. laevis*. Synthetic mRNAs were transcribed from either pGEM3 or pGEM3Zf(+) encoding the wt $M_2$ or mutant $M_2$ proteins and were microinjected (50 nl of RNA of 1 μg/μl) into oocytes of *X. laevis*. At 24 h postinjection, oocytes were labeled with [$^{35}$S]methionine and homogenized, and detergent lysates were prepared in the presence of 50 mM iodoacetamide. Proteins were immunoprecipitated with an $M_2$-specific monoclonal antibody (14C2) and analyzed by SDS-PAGE under reducing (B) and nonreducing (C) conditions. M, influenza virus-infected CV-1 cell lysate used as molecular size markers; HA = 77 kDa, NP = 56 kDa, $M_1$ = 28 kDa, and $M_2$ = 15 kDa. Positions of the $M_2$ monomer, dimer, and tetramer bands (15, 30, and 60 kDa, respectively) are shown on the right.

current associated with expression of $M_2$ V27A, V27S, A30T, S31N, and G34E remained resistant to the drug (Table 1). For the Udorn $M_2$ protein, the change V27S leads to amantadine resistance, whereas the mutant containing the change V27T was sensitive to amantadine at both pH 7.5 and pH 6.2 (Table 1).

When the pH sensitivities of the membrane currents of oocytes expressing the wt and mutant $M_2$ proteins were compared over the pH range from 7.5 to 5.4, it was found that mutants $M_2$ V27A, V27S, V27T, and S31N had similar slopes of pH activation (Fig. 3). Mutant A30T was only weakly pH activated in comparison with wt $M_2$ protein ion channel activity over the entire pH range, and as discussed above, no significant ion channel activity could be measured for mutant A30P. A statistical analysis using a two-way analysis of variance (ANOVA) indicated that the pH activations of $M_2$ A30P and A30T were significantly different from each other and from those of all other proteins (ANOVA: $F = 12.49$; $P < 0.0001$).

**Specific activity of wt and mutant $M_2$ protein channel currents in oocytes.** Oocytes expressing various $M_2$ mutants

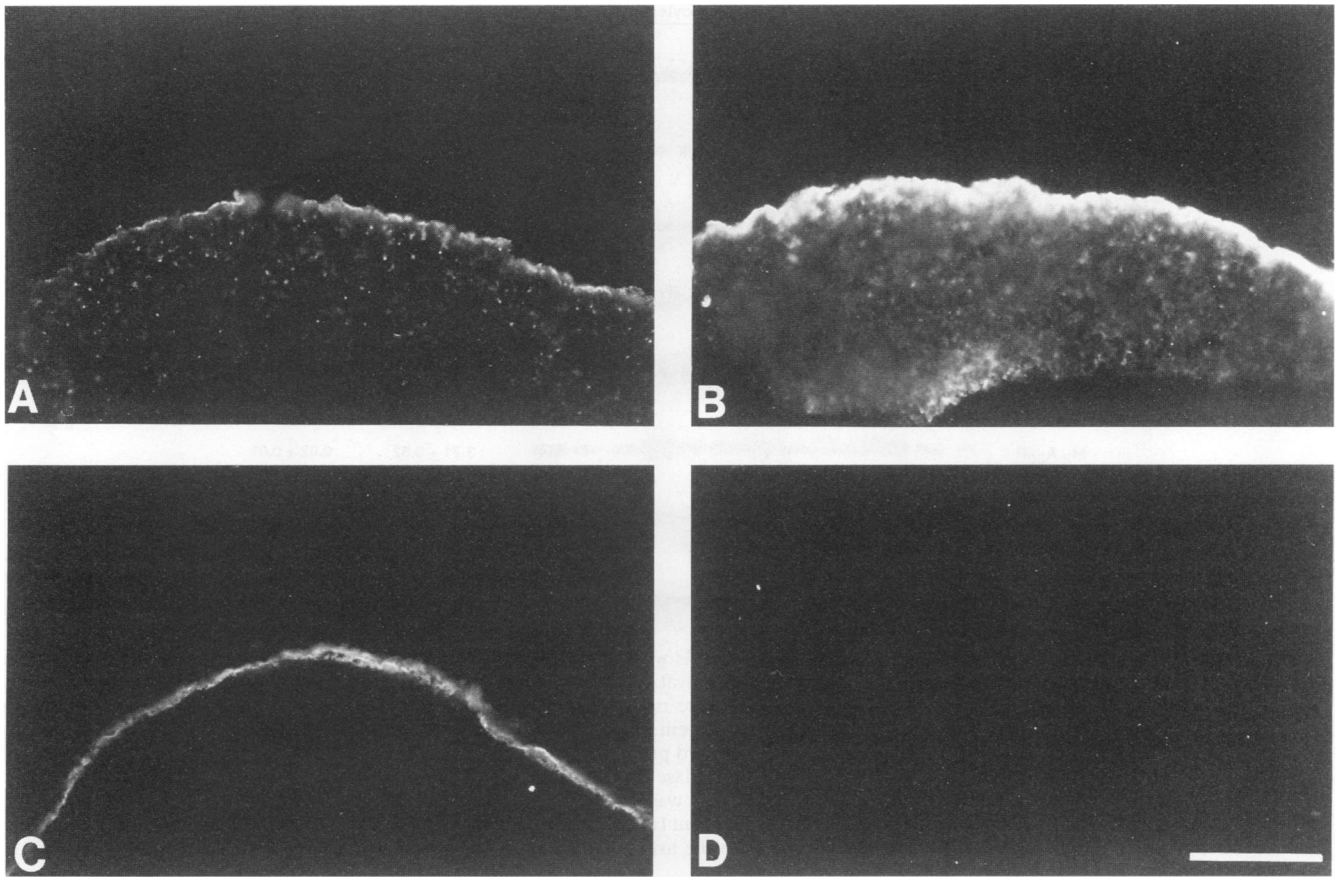


FIG. 2. Cell surface expression of mutant $M_2$ proteins expressed in oocytes of *X. laevis*. Indirect immunofluorescence microscopy of sections of oocytes was performed as described in Materials and Methods. The $M_2$ protein was stained with the $M_2$-specific monoclonal antibody 14C2 followed by FITC-conjugated goat anti-mouse secondary antibody. (A) $M_2$ V27T; (B) $M_2$ A30P; (C) $M_2$ G34E; (D) injection of antisense RNA. Photographic exposure times were equivalent. Bar, 100 μm.

exhibited different levels of whole-cell currents. This could reflect an intrinsic property of the channel per se or a variation in expression levels between oocytes. To distinguish between these possibilities, the peak amplitude of inward current of individual oocytes was measured following an activating voltage of −130 mV in Barth's solution (pH 6.2). The oocyte was then lysed, and the amount of $M_2$ protein that had accumu-

TABLE 1. Amplitudes of inward currents

| $M_2$ protein genotype | Inward current (μA) (mean ± SEM)[a] | | | *n* |
|---|---|---|---|---|
| | pH 7.5 | pH 6.2 | pH 6.2 + 100 μM amantadine | |
| WT | 0.13 ± 0.04 | 0.73 ± 0.13 | 0.06 ± 0.03[b] | 5 |
| V27A | 0.27 ± 0.04 | 1.09 ± 0.12 | 0.87 ± 0.10 | 6 |
| V27S | 0.23 ± 0.06 | 0.71 ± 0.08 | 0.70 ± 0.09 | 6 |
| V27T | 0.06 ± 0.01 | 0.60 ± 0.08 | 0.02 ± 0.01[b] | 10 |
| A30T | 0.09 ± 0.01 | 0.23 ± 0.02 | 0.25 ± 0.02 | 5 |
| A30P | 0.03 ± 0.01 | 0.04 ± 0.01 | 0.05 ± 0.01 | 9 |
| S31N | 0.08 ± 0.01 | 0.78 ± 0.06 | 0.55 ± 0.04 | 6 |
| G34E | 0.06 ± 0.01 | 0.61 ± 0.08 | 0.75 ± 0.08 | 10 |
| W41A | 0.03 ± 0.01 | 0.05 ± 0.02 | 0.00 ± 0.01 | 5 |

[a] Current of control oocytes injected with antisense RNA (endogenous current) was subtracted from total current measured to yield current reported. Currents were measured at −130 mV.

[b] Reduced by amantadine, $P < 0.01$.

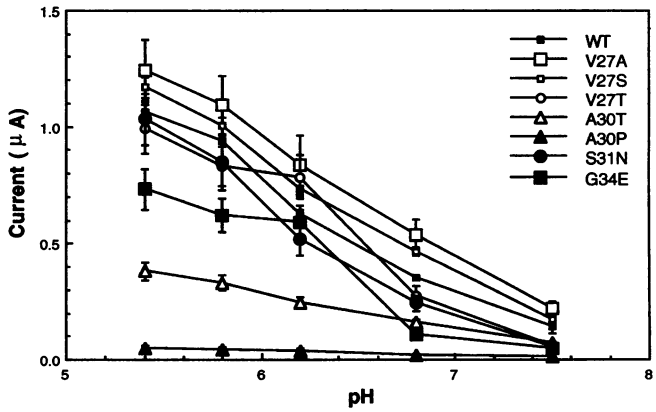


FIG. 3. Modulation of membrane currents of oocytes expressing the wt $M_2$ and mutant $M_2$ proteins by pH. Oocytes were microinjected with synthetic RNA transcripts encoding the mutant $M_2$ proteins. Electrophysiological measurements were performed at 40 to 50 h postinjection. The peak amplitude of inward currents following a hyperpolarizing pulse of −130 mV for the indicated $M_2$ protein is plotted against extracellular pH. In this and subsequent figures, background endogenous currents recorded from oocytes injected with antisense RNA were subtracted from each datum point, as described in Table 1, footnote *a*. Two-way ANOVA was done as described in Materials and Methods.

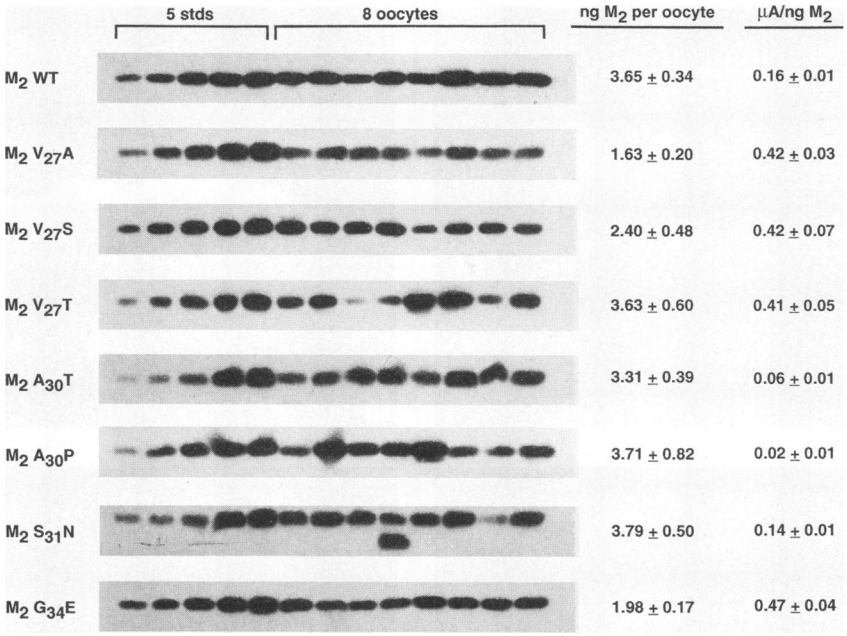


FIG. 4. Normalization of wt $M_2$ and mutant $M_2$ expression levels with ion channel currents indicates that different channels have distinct properties. The peak amplitude of current following a −130-mV activating voltage at pH 6.2 was measured for eight individual oocytes for each mutant $M_2$ protein. Each oocyte was then homogenized, lysates were run on SDS-PAGE, and polypeptides were transferred to polyvinylidene difluoride membranes. Five known concentrations of purified $M_2$ protein were coelectrophoresed with mutant $M_2$ protein so that the accumulated $M_2$ protein in oocytes could be quantified. The amount of the standard purified $M_2$ protein varied for each mutant $M_2$ protein. Blots were probed with $M_2$-specific monoclonal antibody 14C2 and horseradish peroxidase-conjugated secondary antibody, and immune complexes were detected with the ECL system. Quantitation of $M_2$ protein in individual oocytes was done by laser scanning densitometry of the X-ray films, using the known concentrations of purified $M_2$ to generate a standard curve. The current (mean ± standard error of the mean) at pH 6.2 in microamps was divided by the total amount (nanograms) of protein for each oocyte, and the average $M_2$ protein specific activity for six oocytes is reported.

lated in each oocyte was quantified by an immunoblotting procedure using 50 to 400 pg of immunoaffinity-purified $M_2$ protein as a standard in order to normalize the whole-cell currents to the amount of accumulated protein, which here is defined as the specific activity. The precise amounts of standard $M_2$ protein used varied depending on the mutant under analysis. The immunoblot analysis of eight individual oocytes and the average specific activity of each mutant, expressed as microamps of current at pH 6.2 per nanogram of $M_2$ protein expressed, is shown in Fig. 4. Mutants V27A, V27S, V27T, and G34E had an increased specific activity (0.41 to 0.47 μA/ng of $M_2$ protein) compared with wt $M_2$ (0.16 μA/ng). S31N was similar to wt $M_2$ (0.14 μA/ng), A30T had a greatly reduced but detectable activity (0.06 μA/ng), and A30P had virtually no activity (0.02 μA/ng).

**Analysis of altered $M_2$ proteins that are modified by addition of N-linked carbohydrate.** When an altered protein, $M_2$+V, A30T, that contains an addition of a valine residue between $M_2$ residues 26 and 29 in addition to the change A30T, was expressed in oocytes, it was found on SDS-PAGE analysis that in addition to the $M_2$ (~15-kDa) band, an additional band ($M_{2g}$; ~18 kDa) and heterogeneously migrating species ($M_{2p}$; ~30 to 50 kDa) could be detected (32) (Fig. 5B). When the ion channel activity of $M_2$+V, A30T was examined, it was found to have altered kinetic and voltage-dependent activation properties (32). We were interested in investigating whether the altered mobilities of the additional species on SDS-PAGE were due to the addition of N-linked carbohydrate and also the possible role of carbohydrate addition in the altered ion channel activity of $M_2$+V, A30T.

Oocytes were coinjected with RNA encoding $M_2$+V, A30T and tunicamycin, the inhibitor of N-linked carbohydrate addition, and when polypeptides were examined on SDS-PAGE, only the 15-kDa unglycosylated band was detected (Fig. 5B). The heterogeneously migrating $M_{2p}$ species was reminiscent of the pattern observed for modification of the carbohydrate chains of the NB glycoprotein of influenza B virus by addition of polylactosaminoglycan (42, 43). Thus, oocyte lysates expressing $M_2$+V, A30T were digested with endo-β-galactosidase, which specifically digests polylactosaminoglycan. As shown in Fig. 5B, the heterogeneously migrating material was no longer observed, and concomitantly, there was an increase in the amount of the $M_{2g}$ species. In addition, some species migrating slightly more slowly than $M_{2g}$ were observed which probably represent trianternary and tetra-antenary cores with lactosaminyl chains not completely digested by endo-β-galactosidase. Thus, these data indicate that some of the $M_2$+V, A30T molecules are modified by addition of N-linked carbohydrate chains (species $M_{2g}$), and these chains are further modified by addition of polylactosaminoglycan (species $M_{2p}$).

Wild-type $M_2$ protein contains a potential site for the addition of N-linked carbohydrate (NDS; residues 20 to 22) which is not used in wt $M_2$ protein (24, 45). To provide evidence that this consensus sequence site is used for carbohydrate addition in $M_2$+V, A30T, two independent mutations, N20S and S22A, were introduced into the $M_2$+V, A30T molecule, each of which would be expected to abolish N-linked carbohydrate addition. As shown in Fig. 5B, when the molecules $M_2$+V, A30T-N20S and $M_2$+V, A30T-S22A were expressed in oocytes, only the unglycosylated $M_2$ species (~15 kDa) was detected, indicating that the asparagine at $M_2$ residue 20 can be modified by addition of carbohydrate.

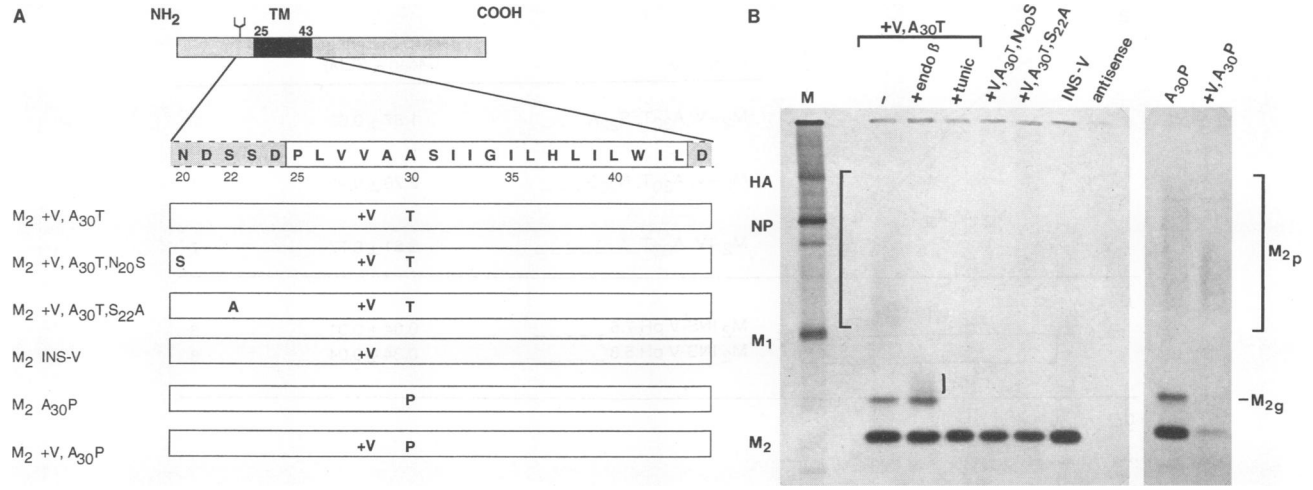


FIG. 5. Construction and expression of mutant $M_2$ proteins to investigate the site of N-linked carbohydrate addition to $M_2$+V, A30T. (A) Schematic diagram of the influenza virus $M_2$ protein and its hydrophobic TM domain residues 25 to 43. The amino acid sequence of the regions flanking the TM domain and the TM domain are shown in the expanded section of the diagram, using the single-letter code. The mutants $M_2$+V, A30T; $M_2$+V, A30T-N20S; $M_2$+V, A30T-S22A; $M_2$-INS-V; $M_2$ A30P, and $M_2$+V, A30P were constructed as described in Materials and Methods. Residues 20 to 22 (NDS) form a consensus sequence for addition of N-linked carbohydrate and are indicated on the schematic diagram of the $M_2$ protein by the tree symbol. All mutants with the designation +V contain an insertion of a valine residue between residues 26 and 29. (B) Expression of mutant $M_2$ proteins in oocytes of *X. laevis*. Synthetic RNAs encoding mutant $M_2$ proteins were microinjected (50 nl of RNA of 1 μg/μl) into oocytes of *X. laevis*. At 24 h postinjection, oocytes were labeled with [$^{35}$S]methionine and homogenized in detergent buffer. Proteins were immunoprecipitated with an $M_2$-specific monoclonal antibody (14C2) and analyzed by SDS-PAGE in the presence of the reducing agent DTT. Lanes: M, marker lane of influenza virus-infected cell proteins as described in the legend to Fig. 1; +tunic, oocytes coinjected with $M_2$+V, A30T RNA and tunicamycin; +endo β, $M_2$+V, A30T protein digested with endo-β-galactosidase; antisense, oocyte injected with antisense $M_2$ RNA. $M_{2p}$ denotes $M_2$ containing heterogeneous glycan additions (polylactosaminoglycan). The small bracket indicates the altered form of $M_{2p}$ after endo-β-galactosidase digestion. $M_{2g}$ denotes $M_2$ containing one high-mannose carbohydrate chain.

To investigate whether the addition of a valine residue alone promoted the addition of N-linked carbohydrate, the mutant $M_2$-INS-V (valine added between residues 26 and 29) was expressed in oocytes. As shown in Fig. 5B, no evidence of a glycosylated $M_2$-INS-V species was found. When $M_2$ A30P was expressed, a mixture of unglycosylated $M_2$, $M_{2g}$, and $M_{2p}$ was observed (Fig. 1B and 5B). Addition of a valine residue between residues 26 and 29 into A30P increased the ratio of glycosylated to unglycosylated species (Fig. 5B). Taken together, these data suggest that perturbations to the $M_2$ TM domain make the site accessible to oligosaccharyltransferase for N-linked carbohydrate addition.

**Ion channel activity of glycosylated and unglycosylated $M_2$ proteins.** Oocytes expressing the glycosylated $M_2$+V, A30T protein exhibited an ion channel activity that is resistant to block by amantadine, is voltage activated, and has two kinetic components: one which appears immediately after the application of the hyperpolarizing voltage and a second which increases with time (32) (Fig. 6). Thus, it was possible to test whether glycosylation provided an explanation for the different properties of $M_2$+V, A30T channel activity from wt $M_2$. Oocytes expressing the mutants $M_2$+V, A30T; $M_2$+V, A30T-N20S; $M_2$+V, A30T-S22A; $M_2$-INS-V; $M_2$-A30P; and $M_2$+V, A30P, when examined by immunochemistry, exhibited bright plasma membrane staining for $M_2$ protein (data not shown), indicating transport of the proteins to the plasma membrane. When the ion channel activities of glycosylated $M_2$+V, A30T and unglycosylated $M_2$+V, A30T-N20S and $M_2$+V, A30T-S22A were tested by using an activation voltage of either −130 or −140 mV, all three proteins exhibited similar time-dependent voltage-activated currents that had two kinetic components (Fig. 6; only the profile of $M_2$+V, A30T is shown). The peak amplitudes of the inward currents from all three proteins were similar following an activation voltage pulse of −130 mV (Fig. 6). Thus, these data suggest that the addition of N-linked carbohydrate to $M_2$+V, A30T does not play a role in the formation of the altered ion channel activity. Interestingly, $M_2$-INS-V when expressed in oocytes did not exhibit voltage-activated ion channel activity but rather exhibited a time-independent, amantadine-sensitive (data not shown), pH-activated current (Fig. 6)—the hallmarks of wt $M_2$. Neither $M_2$ A30P nor $M_2$+V, A30P exhibited detectable ion channel activity (data not shown). Thus, taken together, the data suggest that it is the presence of the A30T change, in conjunction with the addition of the extra valine residue, that leads to the altered ion channel properties.

**Ion channel activities and oligomeric structures of $M_2$ proteins containing deletions in the TM domain.** An amantadine-resistant mutant of FPV Weybridge was found to contain a deletion of four residues (residues 28 to 31) in the $M_2$ protein TM domain (12). We introduced this deletion into the Udorn $M_2$ protein ($M_2$ $del_{28-31}$), and when $M_2$ $del_{28-31}$ was expressed in oocytes, an amantadine-resistant, voltage-activated inward current was observed (32). We were interested in examining whether other deletions in the $M_2$ protein TM domain could yield a viable $M_2$ channel activity. Two mutants in which three or five residues were deleted from the TM domain were constructed and expressed in oocytes; these mutants were designated $M_2$ $del_{29-31}$ and $del_{27-31}$, respectively (Fig. 7). Whereas oocytes expressing $M_2$ $del_{28-31}$ exhibited a large inward current independent of extracellular pH, oocytes expressing either $M_2$ $del_{29-31}$ or $M_2$ $del_{27-31}$ exhibited currents that were not significantly larger than those of control oocytes injected with antisense RNA (Fig. 7). To determine whether the lack of ion channel activity was due to a failure of $M_2$ $del_{29-31}$ or $del_{27-31}$ to be expressed at the oocyte plasma

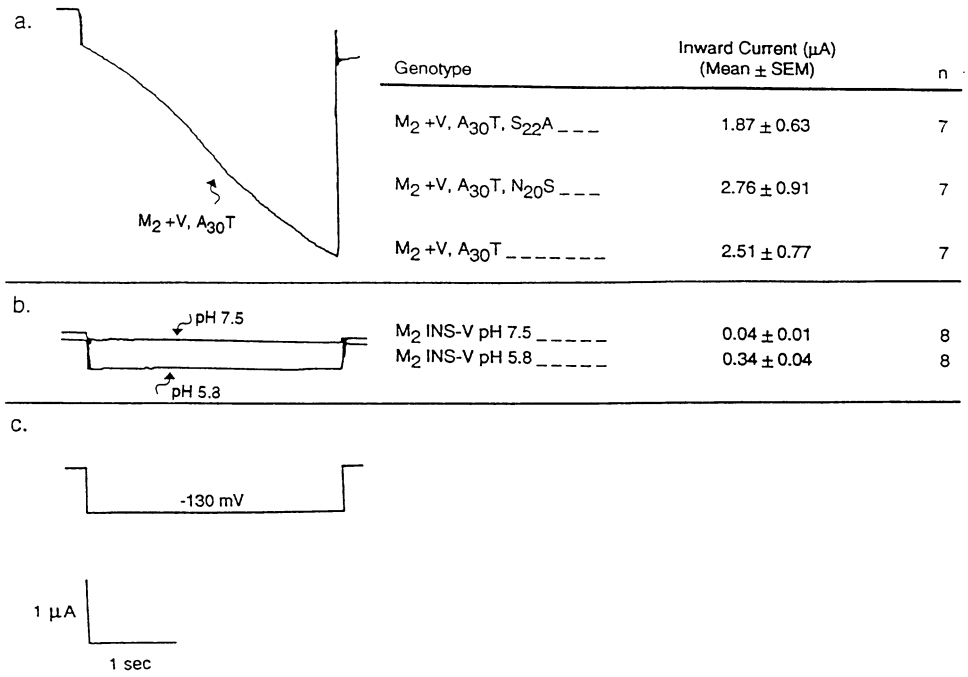


FIG. 6. Analysis of the amplitude and time course of currents associated with glycosylated and unglycosylated mutant $M_2$ proteins. (a) Left, time dependence of the currents associated with $M_2$+V, A30T; $M_2$+V, A30T-S22A; and $M_2$+V, A30T-N20S on a hyperpolarizing voltage step to −130 mV (time course in panel c). Only the current profile of $M_2$+V, A30T is shown as an example of the three voltage-activated currents. Right, peak current amplitudes during an activating voltage to −130 mV for oocytes expressing the mutants shown. (b) Left, time independence of the currents associated with $M_2$-INS-V at pH 7.5 and 5.8; right, peak current amplitudes during an activating voltage to −130 mV for oocytes expressing $M_2$-INS-V. (c) Time course of hyperpolarization, current scale, and time scale for panels a and b.

membrane, immunochemistry for $M_2$ was performed. As shown in Fig. 8, a bright $M_2$-specific plasma membrane staining was observed with $M_2$ $del_{29-31}$ and $del_{28-31}$. However, oocytes expressing $M_2$ $del_{27-31}$ showed only very low levels of $M_2$-specific plasma membrane staining, which suggests that this mutant was poorly transported to the cell surface or did not accumulate at the cell surface.

The lack of $M_2$-specific surface fluorescent staining for $M_2$ $del_{27-31}$ could be due to a failure of the protein to oligomerize, thus preventing intracellular transport of the molecule (reviewed in reference 4). Therefore, the $M_2$ TM domain deletion mutant polypeptides were analyzed by SDS-PAGE under reducing (in the presence of DTT) and nonreducing (in the absence of DTT) conditions. As shown in Fig. 9A, under reducing conditions, a ~14-kDa polypeptide species was observed for $M_2$ $del_{27-31}$, $del_{28-31}$, and $del_{29-31}$. Under nonreducing conditions, both $M_2$ $del_{27-31}$ and $M_2$ $del_{29-31}$ formed an approximately equal mixture of disulfide-linked dimers (~28 kDa) and disulfide-linked tetramers (~56 kDa) (Fig. 9A), which is the pattern observed for wt $M_2$ protein (15, 38). Thus, the inability to detect $M_2$ $del_{27-31}$ does not appear to be due to a failure of the protein to oligomerize.

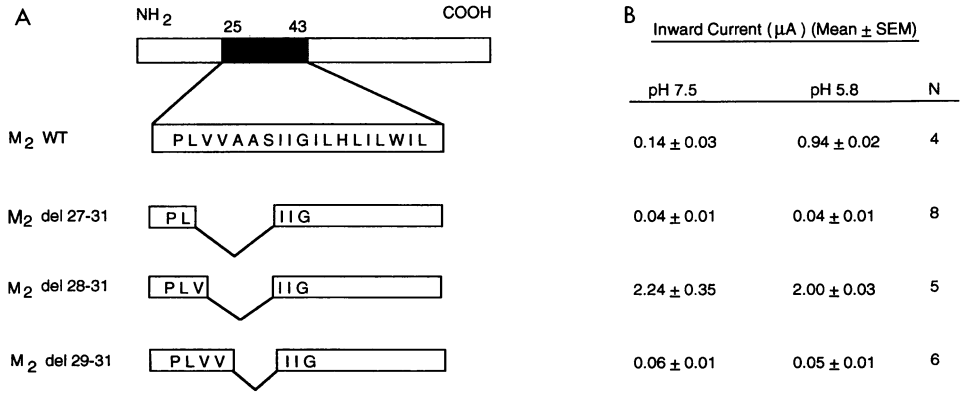


FIG. 7. Analysis of the current associated with $M_2$ proteins containing deletions in the TM domain. (A) Schematic diagram of the $M_2$ TM domain indicating the locations of the deletions in the mutants $M_2$ $del_{29-31}$, $del_{28-31}$, and $del_{27-31}$. These mutants were constructed, and RNA was synthesized and expressed in oocytes, as described in Materials and Methods. (B) Peak current amplitudes during an activating voltage to −130 mV measured at pH 7.5 and 5.8 for each mutant.

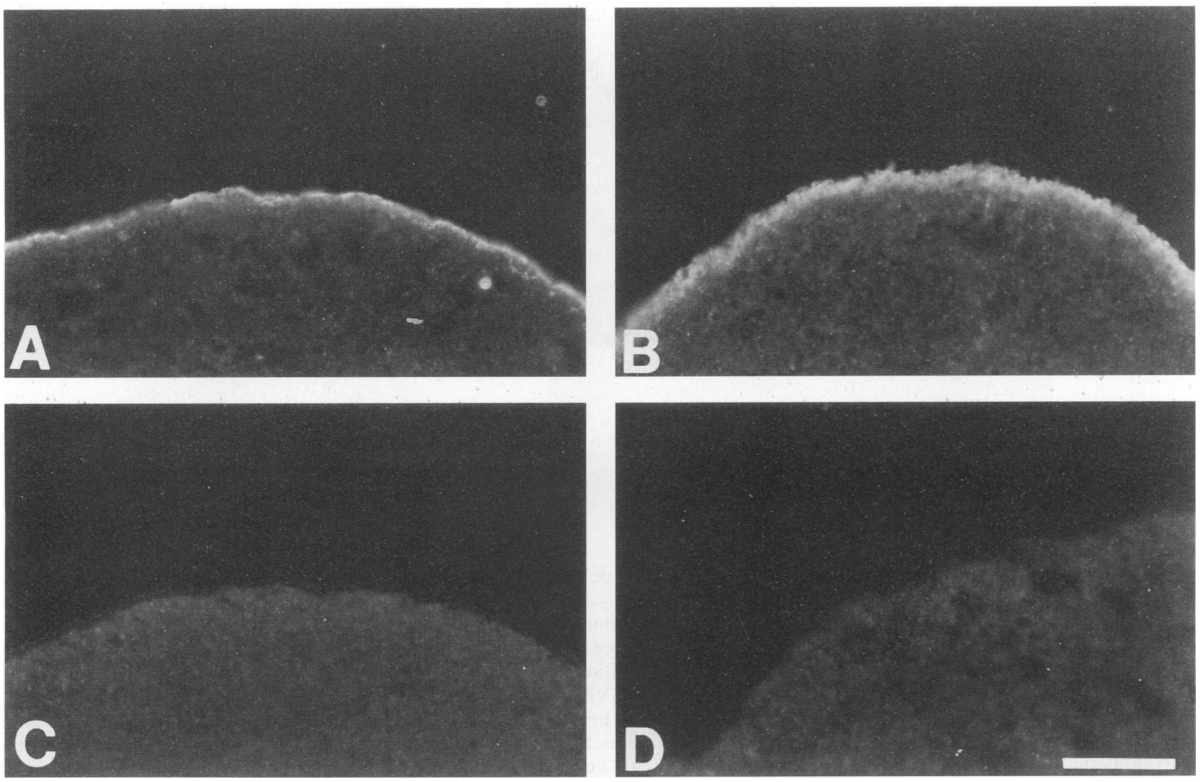


FIG. 8. Cell surface expression of $M_2$ proteins containing membrane-spanning domain deletions expressed in oocytes of *X. laevis*. Indirect immunofluorescence microscopy was done on sections of oocytes stained with $M_2$-specific monoclonal antibody 14C2 followed by FITC-conjugated rabbit anti-mouse secondary antibody as described in Materials and Methods. (A) $M_2$ $del_{28-31}$; (B) $M_2$ $del_{29-31}$; (C) $M_2$ $del_{27-31}$; (D) oocyte injected with antisense RNA. Photographic exposure times were equivalent. Bar, 100 μm.

Most interestingly, $M_2$ $del_{28-31}$, when analyzed by SDS-PAGE under nonreducing conditions, formed, in addition to disulfide-linked dimers and tetramers, two prominent additional species of ~42 and 70 kDa, which are molecular masses that would be predicted for trimeric and pentameric $M_2$ species. To examine further the oligomeric form of $M_2$ $del_{28-31}$, we performed an analysis of $M_2$-$del_{28-31}$ expressed in CV-1 cells, using homobifunctional cross-linking reagents and an SV40 recombinant virus expression system. The $M_2$ $del_{28-31}$ polypeptide species found under nonreducing conditions were the same with either the oocyte or mammalian cell expression system (Fig. 9), but cross-linking is technically simpler with mammalian cells. CV-1 cells expressing either wt $M_2$ or $M_2$ $del_{28-31}$ were lysed, and cross-linking was performed on the whole-cell lysate by using DSP; alternatively, cross-linking was performed on intact cells expressing the $M_2$ protein by using EGS (see Materials and Methods). As shown in Fig. 9B, when wt $M_2$ was analyzed by SDS-PAGE under nonreducing conditions, it was found to be cross-linked predominantly to a ~60-kDa species, as found previously (15). In contrast, $M_2$ $del_{28-31}$ was found to be cross-linked to a species similar in mobility to the largest disulfide-linked species (~70 kDa). To further examine the change in form of the oligomer of $M_2$ $del_{28-31}$ compared with wt $M_2$, DSP-cross-linked $M_2$ $del_{28-31}$ and wt $M_2$ were subjected to sucrose velocity sedimentation. As shown in Fig. 10, the major $M_2$ $del_{28-31}$ oligomeric species sedimented more rapidly than the major wt $M_2$ oligomeric species, which is consistent with $M_2$ $del_{28-31}$ having a larger mass. Thus, these data suggest that the oligomeric form of $M_2$ $del_{28-31}$ is different from the tetrameric wt $M_2$ protein, and the data are consistent with $M_2$ $del_{28-31}$ forming a pentamer with various disulfide bond arrangements between subunits. The altered oligomeric structure of $M_2$ $del_{28-31}$ may be the basis for the different ion channel properties of $M_2$ $del_{28-31}$ compared with wt $M_2$ protein.

## DISCUSSION

In addition to the influenza virus $M_2$ ion channel protein, the only other known ion channel that has a single TM domain is the 130-residue $I_{SK}$ (min K) $K^+$ channel (7, 8, 33, 36, 40), and interestingly, $I_{SK}$, like the $M_2$ protein, is thought to be a type III integral membrane protein. Thus, in comparison with cloned ion channels having a multiple membrane-spanning domain architecture and pores formed by larger oligomeric complexes which share similar structural elements (reviewed in references 17 and 26), the influenza virus $M_2$ protein is a minimalistic or primative ion channel. The small size of the $M_2$ protein makes feasible a structure-function analysis by selectively changing residues in the pore region.

It has been suggested that the $M_2$ protein TM domain adopts an α-helical secondary structure (6, 35, 38). When the TM domain is modeled as an α helix (Fig. 11), residues 27, 30, 31, 34, 37, 38, and 41 are found to be located on the same face of the α helix, and specific changes at residues 27, 30, 31, and 34 lead to an ion channel that is resistant to block by amantadine (9, 12, 32, 41). In addition, we have shown previously that the change H37A results in channel activity that is not pH activated, and the change L38F in the FPV Rostock $M_2$ protein results in a channel activity that is activated by pH

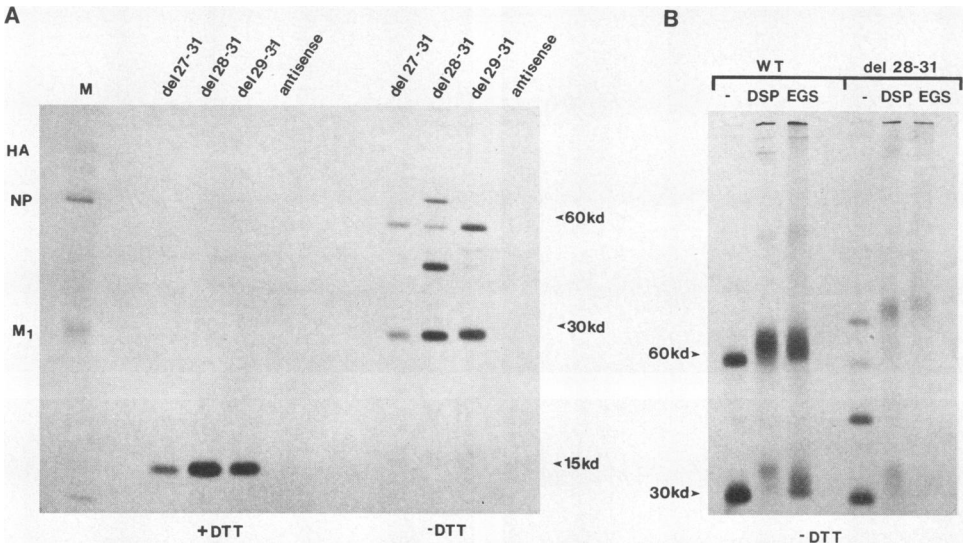


FIG. 9. Analysis of the oligomeric forms of $M_2$ proteins containing deletions in the membrane-spanning domain by chemical cross-linking and SDS-PAGE. (A) Oocytes were injected with the RNAs encoding $M_2$ $del_{27-31}$, $del_{28-31}$, and $del_{29-31}$, labeled with [$^{35}$S]methionine, and homogenized in detergent buffer containing 50 mM iodoacetamide. Proteins were immunoprecipitated with an $M_2$-specific monoclonal antibody (14C2) and analyzed under reducing (+DTT) and nonreducing (−DTT) conditions on a 17.5% polyacrylamide–4 M urea gel. M, marker lane of influenza virus infected-cell proteins as described in the legend to Fig. 1. Positions of the wt $M_2$ monomer, dimer, and tetramer (15, 30, and 60 kDa, respectively) are shown at the right. (B) CV-1 cells infected with SV40 recombinants expressing wt $M_2$ and $M_2$ $del_{28-31}$ were labeled with [$^{35}$S]cysteine from 45 to 48 h postinfection. Cells were then lysed and proteins were cross-linked with DSP (lane DSP), or cell monolayers were incubated with the cross-linker EGS (lane EGS) prior to cell lysis as described in Materials and Methods. Proteins were immunoprecipitated with $M_2$-specific antibody 14C2 and analyzed on a 10% polyacrylamide gel under nonreducing conditions. The predominant cross-linked form of $M_2$ $del_{28-31}$ is denoted by an asterisk. $^{14}$C-labeled molecular weight markers were used as molecular weight standards (not shown).

but is largely resistant to amantadine block (32, 41). Taken together, the data described in this report and those described previously indicate that changing any residue on this face of the putative α helix of the $M_2$ TM domain alters properties of the $M_2$ ion channel.

For the Udorn $M_2$ protein, the changes V27A, V27S, V27T, S31N, and G34E yielded channel activities with pH activation curves that could not be distinguished from that of wt $M_2$, and all showed a quasi-linear slope of activation to pH 5.4, the lowest pH that the oocytes could tolerate and give low currents upon return to pH 7.5. Mutations in $M_2$ proteins A30P and W41A effectively abolished meaningful channel activity at both pH 7.5 and pH 6.2. Thus, although $M_2$ A30P and W41A form tetramers that are expressed at the oocyte plasma membrane, the point mutations resulted in a loss of ion flux. Interestingly, one naturally occurring mutant, A30T, which exhibited a small pH activation response that was distinct from those of all the other mutants tested was found (Fig. 3 and Table 1). When the A30T mutation was found in FPV Rostock, virus growth was impaired, and when the virus was passaged in the absence of amantadine, the A30T mutation readily reverted to wt (9). Thus, these in vivo observations suggest pH activation is of great importance to the ion channel function in the influenza virus life cycle.

We observed that oocytes expressing the mutant $M_2$ ion channels had different membrane currents. In addition to a varying pH activation response, a difference in the total cell surface currents of oocytes expressing the $M_2$ proteins could be due to different levels of expression. As all of the point mutants tested could be readily detected at the oocyte plasma membrane, the assumption was made that the total $M_2$ protein accumulation in oocytes, as determined by a quantitative immunoblotting, directly reflected the surface expression levels. Calculation of the specific activity of these $M_2$ ion channel activities (microamps per nanogram of $M_2$) indicated that in comparison with wt $M_2$, the $M_2$ S31N mutation had a neutral effect, whereas $M_2$ molecules containing the changes V27A, V27S, V27T, and G34E had a 2.5-fold increase in activity over wt $M_2$. In contrast $M_2$ A30T, which is only weakly pH activated, had a specific activity 2.5-fold lower than that of wt $M_2$. The calculation of the specific activity of the $M_2$ ion channels is a useful measurement; however, until single-channel recordings are made, we cannot distinguish whether the channel currents vary in activity due to changes in ion flux, due to changes in the fraction of time that each individual channel spends in the open state, or due to the fraction of molecules that do not enter into an active ion channel complex.

The $M_2$-mediated alteration in the conformational form of HA (either low-pH or native form) was used as an assay of the activities of the FPV Rostock, FPV Weybridge, and Udorn $M_2$ proteins in mammalian cells (9, 10, 39). The data obtained indicate that the ion channel activity of FPV Rostock $M_2$ is more active than that of either the FPV Weybridge or Udorn $M_2$ protein. In addition, by using FPV Rostock and FPV Weybridge point mutations conferring amantadine resistance, it was found that the primary structure of the whole $M_2$ TM domain influenced the consequence of specific residue changes. For example, the change G34E in FPV Rostock $M_2$ protein was found to diminish $M_2$ protein activity, whereas the G34E change in FPV Weybridge $M_2$ protein was found to increase the $M_2$ protein activity (9). Our estimates of ion channel specific activity, by measuring the whole-cell currents of oocytes expressing $M_2$ proteins with changes in the TM domain as a function of $M_2$ protein expression levels, lend further support to the notion that there is a complex relationship between the role of a specific residue at a particular

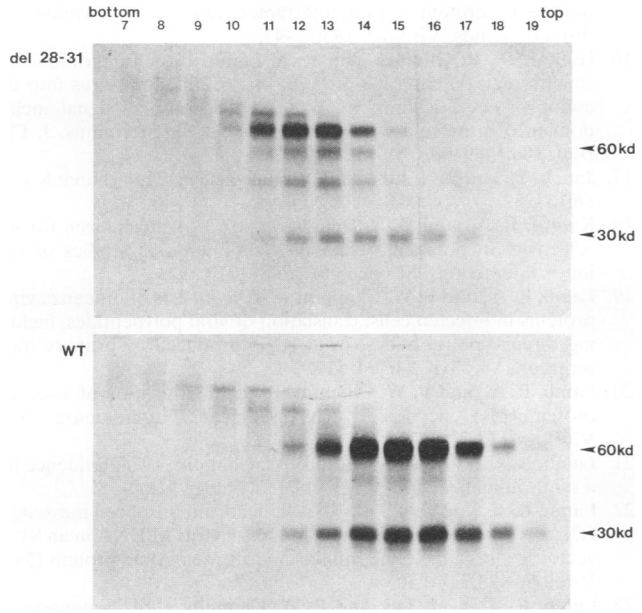


FIG. 10. Sucrose density gradient analysis of the oligomeric forms of the wt $M_2$ and $M_2$ $del_{28-31}$ proteins. CV-1 cells were infected with SV40 recombinants expressing wt $M_2$ or $M_2$ $del_{28-31}$, labeled with [$^{35}$S]cysteine from 45 to 48 h postinfection, and lysed in Triton X-100–MNT buffer containing 50 mM iodoacetamide. Proteins were cross-linked with DSP as described in Materials and Methods, and lysates were subjected to sucrose velocity sedimentation on 5 to 15% sucrose gradients (38,000 rpm, 24 h, 20°C in an SW41 rotor). Twenty-four 0.5-ml fractions were collected from the bottom of each gradient, the indicated fractions were immunoprecipitated with $M_2$-specific monoclonal antibody 14C2, and polypeptides were analyzed on a 17.5% polyacrylamide–4 M urea gel under nonreducing conditions. $^{14}$C-labeled molecular weight markers were used as molecular weight standards (not shown).


FIG. 11. Helical net projection of the postulated α helix of the $M_2$ protein membrane-spanning domain. Amino acid residues 25 to 43 are shown beginning at the bottom of the helix and winding upward. Residues which lie on one face of the α helix and which affect both ion channel activity and amantadine sensitivity are darkly shaded. The histidine residue involved directly or indirectly in modulation of channel activity by pH is shown lightly shaded.

position in the $M_2$ ion channel and the overall molecular architecture of the $M_2$ ion channel. For example, in both FPV Rostock and FPV Weybridge, the change S31N lowers $M_2$ protein activity, but with Udorn $M_2$ protein, it leads to amantadine resistance with little change in ion channel specific activity. In contrast, the change A30P in FPV Weybridge leads to a viable virus (12), whereas the change A30P in Udorn $M_2$ protein effectively abolishes ion channel activity. In addition, when $M_2$ residue 27 in FPV Rostock is threonine, it leads to amantadine resistance, whereas the presence of threonine in the equivalent position in Udorn $M_2$ protein leads to channel activity that is amantadine sensitive.

It had been shown previously that oocytes expressing the mutant $M_2$+V, A30T, which contains an additional valine residue inserted between residues 26 and 29 and the change A30T, exhibited a voltage-activated ion channel activity that consisted of two kinetic components: one immediately upon hyperpolarization and the second increasing slowly with time. In addition, it was found that $M_2$+V, A30T was susceptible to modification by addition of carbohydrate (32). Our analysis described here indicates that $M_2$ asparagine residue 20 is the site of addition of an N-linked carbohydrate chain and that this chain is further modified by addition of polylactosaminoglycan. However, neither addition of the carbohydrate nor addition of the extra valine residue to the TM domain provides an explanation for the altered current time course, which appears to be dependent on both the change of A30T and the addition of the valine residue. The simplest explanation for the addition of a carbohydrate to the mutants $M_2$+V, A30T; $M_2$ A30P; and $M_2$+V, A30P at asparagine residue 20, which is not modified in wt $M_2$, is that the mutations cause a perturbation in the structure of the TM domain such that asparagine at residue 20 becomes accessible to the oligosaccharyltransferase. Digestion of the heterogeneously migrating $M_2$ species with endo-β-galactosidase is a characteristic of polylactosaminoglycan modification, and in three viral glycoproteins in which this modification has been observed ($M_2$ protein described here, NB of influenza B virus [42, 43], and 1A of respiratory syncytial virus [1, 29]), the glycosylation sites are membrane proximal.

We were intrigued that a naturally selected amantadine-resistant mutant of FPV Weybridge contained a deletion of four residues in the TM domain. When this deletion was made in the Udorn $M_2$ protein ($M_2$ $del_{28-31}$) and expressed in oocytes, it exhibited a voltage-activated (and pH-independent) ion channel activity (32). On hyperpolarization of oocyte membranes to −130 mV, the specific activity of $M_2$ $del_{28-31}$ (1.20 ± 0.30 [mean ± standard error of the means] μA/ng of $M_2$ protein, data not shown) was much greater than that of Udorn wt $M_2$. However, in the in vivo assay measuring the $M_2$-mediated alteration in the conformational form of HA, the data indicated that $M_2$ $del_{28-31}$ was 25-fold less active than FPV Rostock $M_2$ protein and 5-fold less active than Udorn $M_2$ protein (39). A simple explanation for these observations is that in mammalian cells, the natural activating membrane voltage is not as negative as that which we applied artificially across the oocyte membrane. To investigate further the ability of the $M_2$ ion channel protein to tolerate deletions in this region of the TM domain, a deletion of five residues ($M_2$ $del_{27-31}$) and a deletion of three residues ($M_2$ $del_{29-31}$) were made. $M_2$ $del_{27-31}$ was not expressed at the oocyte plasma membrane, and thus no ion channel activity could be measured. $M_2$ $del_{27-31}$ contains a TM domain of only 15 residues, and although it forms a tetramer, we have not investigated the mechanism for the lack of cell surface expression. $M_2$ $del_{29-31}$ formed a tetramer and was readily detected at the oocyte plasma membrane. $M_2$ $del_{29-31}$ lacked meaningful channel activity, which strongly suggests that a specific structure in the

$M_2$ TM domain exists to form the pore of the channel and deletion of three residues destroys this structure. The deletion of four residues in $M_2$ $del_{28-31}$, approximately one full helical turn, may preserve a part of the wt $M_2$ channel structure. But more important for understanding channel structure, the data obtained concerning the oligomeric form of $M_2$ $del_{28-31}$, by using cross-linking reagents and sucrose density gradient analysis, are consistent with $M_2$ $del_{28-31}$ forming an oligomer that is different from wt $M_2$. The data obtained are those which would be predicted for $M_2$ $del_{28-31}$ forming a pentamer. Understanding further the structure of these two distinct minimalistic channels should shed light on their regulation and mechanisms of ion conductance.

## ACKNOWLEDGMENTS

We thank Margaret Shaughnessy for excellent technical assistance and the members of the Lamb laboratory for many helpful discussions.

This research was supported by Public Health Service research grants AI-20201 (R.A.L) and AI-31882 (L.H.P) from the National Institute of Allergy and Infectious Diseases. R.A.L. is an Investigator of the Howard Hughes Medical Institute.

## REFERENCES

1. **Anderson, K., A. M. Q. King, R. A. Lerch, and G. W. Wertz.** 1992. Polylactosaminoglycan modification of the respiratory syncytial virus small hydrophobic (SH) protein: a conserved feature among human and bovine respiratory syncytial viruses. Virology **191:**417–430.
2. **Ciampor, F., P. M. Bayley, M. V. Nermut, E. M. A. Hirst, R. J. Sugrue, and A. J. Hay.** 1992. Evidence that the amantadine-induced, $M_2$-mediated conversion of influenza A virus hemagglutinin to the low pH conformation occurs in an acidic trans Golgi compartment. Virology **188:**14–24.
3. **Ciampor, F., C. A. Thompson, S. Grambas, and A. J. Hay.** 1992. Regulation of pH by the $M_2$ protein of influenza A viruses. Virus Res. **22:**247–258.
4. **Doms, R. W., R. A. Lamb, J. K. Rose, and A. Helenius.** 1993. Folding and assembly of viral membrane proteins. Virology **193:** 545–562.
5. **Duff, K. C., and R. H. Ashley.** 1992. The transmembrane domain of influenza A $M_2$ protein forms amantadine-sensitive proton channels in planar lipid bilayers. Virology **190:**485–489.
6. **Duff, K. C., S. M. Kelly, N. C. Price, and J. P. Bradshaw.** 1992. The secondary structure of influenza A $M_2$ transmembrane domain: a circular dichroism study. FEBS Lett. **311:**256–258.
7. **Folander, K., J. Smith, J. Antanavage, C. Bennett, R. B. Stein, and R. Swanson.** 1990. Cloning and expression of the delayed rectifier $I_{SK}$ channel from neonatal rat heart and diethylstilbestrol-primed rat uterus. Proc. Natl. Acad. Sci. USA **87:**2975–2979.
8. **Goldstein, S. A. N., and C. Miller.** 1991. Site-specific mutations in a minimal voltage-dependent $K^+$ channel alter ion selectivity and open-channel block. Neuron **7:**403–408.
9. **Grambas, S., M. S. Bennett, and A. J. Hay.** 1992. Influence of amantadine resistance mutations on the pH regulatory function of the $M_2$ protein of influenza A viruses. Virology **191:**541–549.
10. **Grambas, S., and A. J. Hay.** 1992. Maturation of influenza A virus hemagglutinin—estimates of the pH encountered during transport and its regulation by the $M_2$ protein. Virology **190:**11–18.
11. **Hay, A. J.** 1992. The action of adamantanamines against influenza A viruses: inhibition of the $M_2$ ion channel protein. Semin. Virol. **3:**21–30.
12. **Hay, A. J., A. Wolstenholme, J. J. Skehel, and M. H. Smith.** 1985. The molecular basis of the specific anti-influenza action of amantadine. EMBO J. **4:**3021–3024.
13. **Heginbotham, L., and R. MacKinnon.** 1992. The aromatic binding site for tetraethylammonium ion on potassium channels. Neuron **8:**483–491.
14. **Helenius, A.** 1992. Unpacking the incoming influenza virus. Cell **69:**577–578.
15. **Holsinger, L. J., and R. A. Lamb.** 1991. Influenza virus $M_2$ integral membrane protein is a homotetramer stabilized by formation of disulfide bonds. Virology **183:**32–43.
16. **Hull, J. D., R. Gilmore, and R. A. Lamb.** 1988. Integration of a small integral membrane protein, $M_2$, of influenza virus into the endoplasmic reticulum: analysis of the internal signal-anchor domain of a protein with an ectoplasmic $NH_2$ terminus. J. Cell Biol. **106:**1489–98.
17. **Jan, L. Y., and Y. N. Jan.** 1989. Voltage-sensitive ion channels. Cell **56:**13–25.
18. **Kumpf, R. A., and D. A. Dougherty.** 1993. A mechanism for ion selectivity in potassium channels: computational studies of cation-$\pi$ interactions. Science **261:**1708–1710.
19. **Lamb, R. A., and P. W. Choppin.** 1976. Synthesis of influenza virus proteins in infected cells: translation of viral polypeptides, including three P polypeptides, from RNA produced by primary transcription. Virology **74:**504–519.
20. **Lamb, R. A., and P. W. Choppin.** 1981. Identification of a second protein ($M_2$) encoded by RNA segment 7 of influenza virus. Virology **112:**729–737.
21. **Lamb, R. A., P. R. Etkind, and P. W. Choppin.** 1978. Evidence for a ninth influenza viral polypeptide. Virology **91:**60–78.
22. **Lamb, R. A., and C.-J. Lai.** 1982. Spliced and unspliced messenger RNAs synthesized from cloned influenza virus M DNA in an SV40 vector: expression of the influenza virus membrane protein ($M_1$). Virology **123:**237–256.
23. **Lamb, R. A., C.-J. Lai, and P. W. Choppin.** 1981. Sequences of mRNAs derived from genome RNA segment 7 of influenza virus: colinear and interrupted mRNAs code for overlapping proteins. Proc. Natl. Acad. Sci. USA **78:**4170–4174.
24. **Lamb, R. A., S. L. Zebedee, and C. D. Richardson.** 1985. Influenza virus $M_2$ protein is an integral membrane protein expressed on the infected-cell surface. Cell **40:**627–633.
25. **Laskey, R. A., and A. D. Mills.** 1975. Quantitative film detection of $^3H$ and $^{14}C$ in polyacrylamide gels by fluorography. Eur. J. Biochem. **56:**335–341.
26. **Miller, C.** 1992. Hunting for the pore of voltage-gated channels. Curr. Biol. **2:**573–575.
27. **Ng, D. T. W., R. E. Randall, and R. A. Lamb.** 1989. Intracellular maturation and transport of the SV5 type II glycoprotein hemagglutinin-neuraminidase: specific and transient association with GRP78-BiP in the ER and extensive internalization from the cell surface. J. Cell Biol. **109:**3273–3289.
28. **Ohuchi, M. A., A. Cramer, M. Vey, R. Ohuchi, and H.-D. Klenk.** 1994. Rescue of vector-expressed fowl plague virus hemagglutinin in biologically active form by acidotropic and coexpressed $M_2$ protein. J. Virol. **68:**920–926.
29. **Olmsted, R. A., and P. L. Collins.** 1989. The 1A protein of respiratory syncytial virus is an integral membrane protein present as multiple, structurally distinct species. J. Virol. **63:**2019–2029.
30. **Paterson, R. G., and R. A. Lamb.** 1987. Ability of the hydrophobic fusion related external domain of a paramyxovirus F protein to act as a membrane anchor. Cell **48:**441–452.
31. **Paterson, R. G., and R. A. Lamb.** 1990. RNA editing by G-nucleotide insertion in mumps virus P-gene mRNA transcripts. J. Virol. **64:**4137–4145.
32. **Pinto, L. H., L. J. Holsinger, and R. A. Lamb.** 1992. Influenza virus $M_2$ protein has ion channel activity. Cell **69:**517–528.
33. **Pragnell, M., K. J. Snay, J. S. Trimmer, N. J. MacLusky, F. Naftolin, L. K. Kaczmerek, and M. B. Boyle.** 1990. Estrogen induction of a small, putative $K^+$ channel mRNA in rat uterus. Neuron **4:**807–812.
34. **Sanger, F., S. Nicklen, and A. R. Coulson.** 1977. DNA sequencing with chain-terminating inhibitors. Proc. Natl. Acad. Sci. USA **74:**5463–5467.
35. **Sansom, M. S. P., and I. D. Kerr.** 1993. Influenza virus $M_2$ protein: a molecular modelling study of the ion channel. Protein Eng. **6:**65–74.
36. **Sugimoto, T., Y. Tanabe, R. Shigemoto, M. Iwai, T. Takumi, H. Ohkubo, and S. Nakanishi.** 1990. Immunohistochemical study of a rat membrane protein which induces a selective potassium permeation: its localization in the apical membrane portion of epithelial cells. J. Membr. Biol. **113:**39–47.
37. **Sugrue, R. J., G. Bahadur, M. C. Zambon, M. Hall-Smith, A. R.**

**Douglas, and A. J. Hay.** 1990. Specific structural alteration of the influenza haemagglutinin by amantadine. EMBO J. **9:**3469–3476.

38. **Sugrue, R. J., and A. J. Hay.** 1991. Structural characteristics of the $M_2$ protein of influenza A viruses: evidence that it forms a tetrameric channel. Virology **180:**617–624.
39. **Takeuchi, K., and R. A. Lamb.** 1994. Influenza virus $M_2$ protein ion channel activity stabilizes the native form of fowl plague virus hemagglutinin during intracellular transport. J. Virol. **68:**911–919.
40. **Takumi, T., H. Ohkubo, and S. Nakanishi.** 1988. Cloning of a membrane protein that induces a slow voltage-gated potassium current. Science **242:**1042–1045.
41. **Wang, C., K. Takeuchi, L. H. Pinto, and R. A. Lamb.** 1993. The ion channel activity of the influenza A virus $M_2$ protein: characterization of the amantadine block. J. Virol. **67:**5585–5594.
42. **Williams, M. A., and R. A. Lamb.** 1986. Determination of the orientation of an integral membrane protein and sites of glycosylation by oligonucleotide-directed mutagenesis: influenza B virus NB glycoprotein lacks a cleavable signal sequence and has an extracellular $NH_2$-terminal region. Mol. Cell. Biol. **6:**4317–4328.
43. **Williams, M. A., and R. A. Lamb.** 1988. Polylactosaminoglycan modification of a small integral membrane glycoprotein, influenza B virus NB. Mol. Cell. Biol. **8:**1186–1196.
44. **Zebedee, S. L., and R. A. Lamb.** 1988. Influenza A virus $M_2$ protein: monoclonal antibody restriction of virus growth and detection of $M_2$ in virions. J. Virol. **62:**2762–2772.
45. **Zebedee, S. L., C. D. Richardson, and R. A. Lamb.** 1985. Characterization of the influenza virus $M_2$ integral membrane protein and expression at the infected-cell surface from cloned cDNA. J. Virol. **56:**502–511.